Mendeleev Communications

Mendeleev Commun., 2025, **35**, 614–616

Ceramic materials based on magnesium orthophosphate for biomedical applications

Ilya I. Preobrazhenskiy,*[a,b] Dina V. Deyneko,[a] Albina M. Murashko,[a] Elena S. Klimashina,[a] Yaroslav Yu. Filippov,[a] Pavel V. Evdokimov[a,c] and Valery I. Putlyaev[a]

[a] *Department of Chemistry, M. V. Lomonosov Moscow State University, 119991 Moscow, Russian Federation. E-mail: preo.ilya@yandex.ru*
[b] *National Research Centre 'Kurchatov Institute', 123182 Moscow, Russian Federation*
[c] *N. S. Kurnakov Institute of General and Inorganic Chemistry, Russian Academy of Sciences, 119991 Moscow, Russian Federation*

DOI: 10.71267/mencom.7716

Magnesium orthophosphate, $Mg_3(PO_4)_2$, was synthesized *via* the solid-phase method, the ceramic material based on $Mg_3(PO_4)_2$ was obtained and the physicochemical properties of the ceramic were studied. The dependence of the changes in the microstructure and density on the sintering temperature in the range of 900 and 1250 °C was investigated.

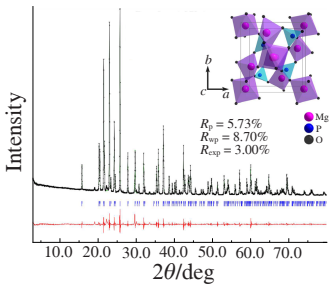

Keywords: magnesium orthophosphate, bioceramics, regenerative medicine, bone defects, microstructure, sintering.

As a result of the increase in the world population, the demand for biomaterials to treat bone defects is growing. 2.8 million bone reconstruction surgeries are performed worldwide every year.[1] Biodegradable materials are the most promising for bone implants because they can be eventually replaced by natural bone tissue, avoiding repeated surgical operations.[2,3] Various materials, comprising ceramics,[4–7] cements,[8–10] polymers[11–13] and composite materials,[14–16] including calcium phosphates, are used to treat the bone defects. The need for biomaterial and limitations of existing implants, such as low bioresorption rate[17] and lack of osteoconductive properties, motivate scientists to develop the new bone regeneration materials. The rate of material dissolution in the body can be controlled by changing its chemical composition.

Over the past few years, magnesium phosphate has attracted interest owing to its potential use in the biomedical field.[18,19] This may be due to the fact that magnesium plays a crucial role in the body as the second most abundant intracellular cation[20] and it is primarily found in the bone tissue, muscle and non-muscle soft tissues (approximately 24 g of Mg per 70 kg of an adult weight).[21] Magnesium phosphate (such as struvite, newberite and calcium-magnesium phosphate) has been found in mineral form in the bones, as well as pathological deposits in kidney stones.[22] The ceramics based on magnesium-substituted calcium phosphate has been studied before, whereas little attention has been paid to pure magnesium phosphate ceramics. Ceramics based on magnesium orthophosphate [$Mg_3(PO_4)_2$] is a promising material, because it is found in the body, in particular, as a part of urinary stones, and it should have good biological properties. Earlier, it was noted that magnesium orthophosphate has specific physical and chemical properties.[23,24] For example, the ceramics with dielectric properties based on $Mg_3(PO_4)_2$ has been developed.[23] In addition, the possibility of using a powder precursor based on this material for 3D printing of bone implants has been shown.[24] However, there is not enough information on the development of techniques to produce ceramics from magnesium phosphates. One of the methods for obtaining magnesium orthophosphate is the solid-phase method. Solutions of $MgCl_2$ and $NH_4H_2PO_4$ salts can be also used as precursors, but it is not possible to precipitate pure crystallohydrate using the solution method. Therefore, the solid-phase method is assumed to be more reliable in the synthesis of this precursor. Thus, the goal of this work was a solid-phase synthesis of $Mg_3(PO_4)_2$, the production of ceramic material and the study of the change of the physicochemical properties of the obtained ceramics depending on the calcination temperature.

For the synthesis of $Mg_3(PO_4)_2$, MgO and $Mg_2P_2O_7$ powders were used. The synthesis of $Mg_3(PO_4)_2$ powder was conducted under reported conditions.[25–27] All reagents used were chemically pure and stored in a dry container. There were no special requirements for handling the initial reagents. The reagents were taken in a stoichiometric ratio. The temperature and calcination duration were chosen on the basis of literature data because they were sufficient for the solid-phase reaction to proceed.

The synthesis of $Mg_3(PO_4)_2$ was carried out using the mechanical activation method. The reaction occurred according to equation (1) at heat treatment temperature of homogenized mixture of MgO and $Mg_2P_2O_7$. After air drying, the product was subjected to heat treatment at a temperature of 1100 °C for 12 h. After that, it was ground in a planetary-type ball mill to produce a powder with a small particle size and then sieved through a Sautilene HiTechTM polyester sieve to disaggregate the resulting mixture and to gain the uniform powder particles.

$$MgO + Mg_2P_2O_7 \rightarrow Mg_3(PO_4)_2 \quad (1)$$

To obtain ceramics, the powders were pressed into tablets by uniaxial one-sided pressing on a Carver C manual press (Carver, USA). Biodegradation of ceramic granules after calcinating at 800 °C and sieving was carried out on an

autotitrator with 0.025 M of citric acid solution. The PXRD patterns were fitted using the STOE WinXPOW software (ICDD PDF-2 database). The relative density of the resulted materials was calculated by the hydrostatic weighing.

The Debye–Scherrer equation[28] was implemented to count the coherent scattering regions (crystallite sizes). LaB6 (SRM 660c) as a line shape standard was applied to determine instrumental broadening. To estimate the contribution of microdeformations, the Williamson–Hall method can be used.[29] Details of the equipment and experimental features are given in Online Supplementary Materials.

According to PXRD data, single-phase pyrophosphate and magnesium oxide were obtained (see Figure S1 in Online Supplementary Materials) after heat-treatment at 1100 °C for 12 h these precursors were used to obtain single-phase magnesium orthophosphate (Figure 1). Basic magnesium carbonate or magnesium oxide obtained by thermal decomposition of magnesium carbonate can be used as one of the initial reagents. The thermal analysis of a mixture of basic magnesium carbonate and magnesium pyrophosphate for the synthesis of magnesium oxide [precursor of $Mg_3(PO_4)_2$ synthesis] is shown in Figure S2 in Online Supplementary Materials. It should be noted that the weight decrease at 450 °C corresponds to the decomposition of magnesium carbonate to form magnesium oxide, which allows one to further use of basic magnesium carbonates as a precursor for obtaining magnesium orthophosphates. Weight reduction at temperatures between 230 and 250 °C is due to the water removal.

In this work, we investigated the possibility of producing ceramics based on $Mg_3(PO_4)_2$. Sintering was performed in an isothermal mode in the range from 900 to 1250 °C for 10 h. PXRD pattern and crystal structures of the synthesized $Mg_3(PO_4)_2$ are presented in Figure 1. According to the Debye–Scherrer equation, the D_{hkl} size for magnesium phosphate was 205 ± 8 nm. The width of the reflex at half height FWHM has a linear dependence on the values of microdeformations and crystallite sizes. However, the contribution of lattice deformation to the broadening of lines on X-ray images is very insignificant in the range of 2θ from 20 to 50°, according to the literature data.[30] The estimation of microdeformations based on the experimental data shows a very small value of 1.28×10^{-5}. Thus, the contribution of microdeformations in the resulting sample can be ignored.

To study the densification processes of the magnesium orthophosphate-based material during heat-treatment, a dilatometric analysis was performed in the range of 900–1250 °C in an isothermal mode for 10 h [Figure 2(*a*)]. According to the literature data and our experiments, there are no phase changes at the temperatures under study.[26] As expected, an increase in temperature results in the enhancement of shrinkage. Thus, at a temperature of 900 °C, shrinkage is practically absent (0.2%). At 950 °C, the shrinkage was 2–2.5%, which apparently corresponds to the initial baking of individual particles. As the temperature

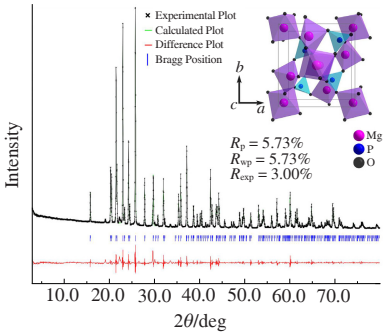

Figure 1 PXRD pattern and crystal structures of the synthesized $Mg_3(PO_4)_2$.

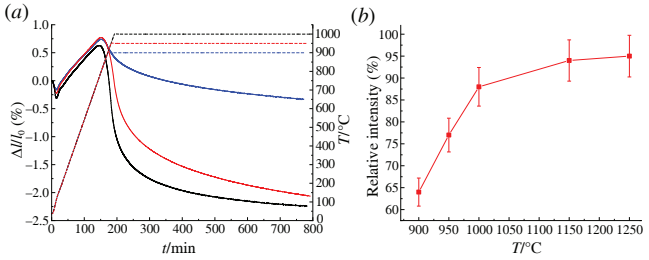

Figure 2 (*a*) Dilatometry results with isothermal exposure for 10 h at 900, 950 and 1000 °C for $Mg_3(PO_4)_2$ and (*b*) relative densities for ceramics based on $Mg_3(PO_4)_2$ sintered at various temperatures.

grows from 1150 to 1200 °C, the shrinkage increases from 7.5 to 10%, which indicates an acceleration of sintering processes. However, a further increase in temperature up to 1250 °C does not cause significant changes, which may suggest that the optimum has been reached at 1200 °C.

The shrinkage values obtained from dilatometry data are given in Table S1 in Online Supplementary Materials. Data on the density of samples measured by hydrostatic weighing [Figure 2(*b*)] point to the significant increase within the temperature range of 900–1000 °C that slows down as the temperature rises to 1150 °C, after which it reaches a plateau. These results agree well with the data of dilatometric measurements, hence, 1150 °C can be considered as optimal for obtaining the dense ceramics under isothermal conditions.

To get the bioceramic implants, it is important to obtain a dense ceramic material, that depends on the choice of sintering temperature. According to SEM data (Figure 3), at 900 °C there is no formation of significant contacts between individual powder particles. This points to the absence of the sintering processes. However, at 1000 °C, the sintering of the individual particles is clearly visible and a large number of pores are present. The appropriate temperature for obtaining the sufficiently dense microstructure without an increase in the average crystallite size was 1150 °C. Raising the heat treatment temperature up to 1250 °C does not completely eliminate pores, but results in their embedding into the volume of crystals, which significantly increases in size compared with the lower sintering temperatures. Based on the above data, it can be concluded that 1150 °C is the optimal temperature for obtaining dense ceramics of the selected composition. As the calcination temperature rises, the grain size and the density of the grain boundaries increase, causing a decrease in the resorption degree of such ceramics.

The study of the ceramic granules resorption was carried out using an auto-titrator at a fixed pH value, which was maintained by adding citric acid during the experiment. When citric acid is added to the solution, an increase in pH values can be seen, which according to the diagram of ionic forms [Figure 4(*a*)] is associated with the dissolution of magnesium orthophosphate, resulting in an increase in magnesium ions, which leads to the formation of newberite ($MgHPO_4{\cdot}3H_2O$). Upon titration of $Mg_3(PO_4)_2$ with citric acid, incongruent dissolution occurs with recrystallization in newberite, which then, dissolving, passes predominantly either as a free magnesium ion or a citrate complex. With an increase in the concentration of citric acid, the predominant form of magnesium in solution changes from Mg^{2+} to $Mg(cit)^-$ at the titration point,

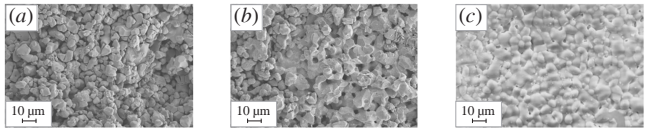

Figure 3 SEM images of ceramics based on $Mg_3(PO_4)_2$ sintered at (*a*) 900, (*b*) 1000 and (*c*) 1150 °C.

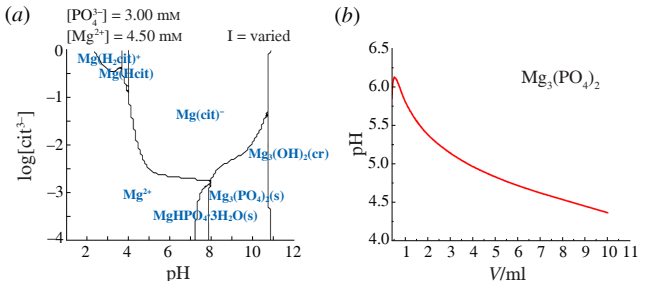

Figure 4 (*a*) Diagram of the predominant ionic and crystalline forms of magnesium in the coordinates of the logarithm of the total concentration of citrate ions *vs.* pH for $Mg_3(PO_4)_2$; (*b*) dissolution kinetics of $Mg_3(PO_4)_2$ ceramic granules on the titrator when adding citric acid.

where $[Mg^{2+}]/[cit^{3-}]$ = 1/1 and cit is $C_3H_5O(COO)_3^{3-}$. Thus, the reaction of dissolution of magnesium orthophosphate in citric acid can be represented as follows:

$$Mg_3(PO_4)_2 + H_3cit \rightarrow 3Mgcit^- + 5H^+ + 2H_2PO_4^- . \quad (2)$$

To study the resorption, ceramic samples in the form of tablets were first prepared by sintering at 800 °C and then they were crushed and sieved through a sieve with a cell size of 220 μm to obtain a homogeneous powder [Figure 4(*b*)]. The amount of acid required to dissolve 0.2 g of $Mg_3(PO_4)_2$ was equal to 9.9 ml. After 24 h, complete dissolution of all ceramic granules was observed. It should be noted that when $Mg_3(PO_4)_2$ ceramic granules were added to a citric acid solution, pH value was equal to 6, which apparently illustrated that this composition would not have a cytotoxic effect on cells.

Thus, when using the solid-phase method to obtain the ceramic materials based on $Mg_3(PO_4)_2$, it has been shown that the most suitable heat treatment temperatures were 1000 and 1150 °C, at which the most dense microstructure was observed and there were no traces of secondary recrystallization. Ceramics obtained at 1100 °C possessed a more dense structure due to the efficiency of the sintering process at this temperature. The relative density of the ceramics produced at 1150 °C was 95 ± 3%. When analyzing the diagram of the predominant ionic and crystalline forms, it was revealed that the dissolution of magnesium orthophosphate in a solution of citric acid occurs incongruently with the formation of newberite. Thus, the ceramic materials based on magnesium orthophosphate, obtained in our work, resorb in a model citric acid solution and may be promising for use as implants for treating bone defects.

This work was supported by the Russian Science Foundation (grant no. 24-29-00396, https://rscf.ru/project/24-29-00396/). A part of the used equipment was purchased through the Program of Lomonosov Moscow State University development.

Online Supplementary Materials

Supplementary data associated with this article can be found in the online version at doi:10.71267/mencom.7716.

References

1 N. Mulchandani, A. Prasad and V. Katiyar, in *Materials for Biomedical Engineering*, eds. V. Grumezescu and A. M. Grumezescu, Elsevier, Amsterdam, 2019, ch. 4, pp. 87–125; https://doi.org/10.1016/B978-0-12-818415-8.00004-8.
2 O. Adekomaya and T. Majozi, in *Bioresorbal Polymers and Their Composites*, eds. D. Verma, K. L. Goh, P. Pasbakhsh, M. Okhawilai, S. Ramakrishna and M. Sharma, Elsevier, Amsterdam, 2024, ch. 2, pp. 23–40; https://doi.org/10.1016/B978-0-443-18915-9.00017-3.
3 T. V. Safronova, *Inorg. Mater.*, 2021, **57**, 443; https://doi.org/10.1134/S002016852105006X.
4 I. V. Fadeeva, A. S. Fomin, S. M. Barinov, G. A. Davydova, I. I. Selezneva, I. I. Preobrazhenskii, M. K. Rusakov, A. A. Fomina and V. A. Volchenkova, *Inorg. Mater.*, 2020, **56**, 700; https://doi.org/10.1134/S0020168520070055.
5 I. V. Fadeeva, D. V. Deyneko, K. Barbaro, G. A. Davydova, M. A. Sadovnikova, F. F. Murzakhanov, A. S. Fomin, V. G. Yankova, I. V. Antoniac, S. M. Barinov, B. I. Lazoryak and J. V. Rau, *Nanomater.*, 2022, **12**, 852; https://doi.org/10.3390/nano12050852.
6 A. K. Nayak, M. Maity, H. Barik, S. S. Behera, A. K. Dhara and M. S. Hasnain, *J. Drug Delivery Sci. Technol.*, 2024, **95**, 105524; https://doi.org/10.1016/j.jddst.2024.105524.
7 S. Luo, Z. Wang, J. He, G. Tang, D. Yuan, Z. Wu, Z. Zou, L. Yang, T. Lu and C. Ye, *Ceram. Int.*, 2024, **50**, 18275; https://doi.org/10.1016/j.ceramint.2024.02.311.
8 I. V. Fadeeva, M. A. Goldberg, I. I. Preobrazhensky, G. V. Mamin, G. A. Davidova, N. V. Agafonova, M. Fosca, F. Russo, S. M. Barinov, S. Cavalu and J. V. Rau, *J. Mater. Sci.: Mater. Med.*, 2021, **32**, 1; https://doi.org/10.1007/s10856-021-06575-x.
9 H. K. Abd El-Hamid, M. M. Farag, M. Abdelraof and R. L. Elwan, *Sci. Rep.*, 2024, **14**, 2804; https://doi.org/10.1038/s41598-024-53319-2.
10 N. A. H. Ahmad, N. B. Husin, N. I. M. Noh and Z. Zakaria, *Mater. Today: Proc.*, 2024, **96**, 73; https://doi.org/10.1016/j.matpr.2023.11.011.
11 I. I. Preobrazhenskiy and V. I. Putlyaev, *Mendeleev Commun.*, 2023, **33**, 83; https://doi.org/10.1016/j.mencom.2023.01.026.
12 I. I. Preobrazhenskii and V. I. Putlyaev, *Russ. J. Appl. Chem.*, 2022, **95**, 775; https://doi.org/10.1134/S1070427222060027.
13 M. J. Javid-Naderi, J. Behravan, N. Karimi-Hajishohreh and S. Toosi, *Polym. Adv. Technol.*, 2023, **34**, 2083; https://doi.org/10.1002/pat.6046.
14 I. V. Fadeeva, D. V. Deyneko, A. V. Knotko, A. A. Olkhov, P. V. Slukin, G. A. Davydova, T. A. Trubitsyna, I. I. Preobrazhenskiy, A. N. Gosteva, I. V. Antoniac and J. V. Rau, *Polymers*, 2023, **15**, 2106; https://doi.org/10.3390/polym15092106.
15 I. I. Preobrazhenskiy, A. A. Tikhonov, P. V. Evdokimov, A. V. Shibaev and V. I. Putlyaev, *Open Ceram.*, 2021, **6**, 100115; https://doi.org/10.1016/j.oceram.2021.100115.
16 S. Peng, X. Yang, W. Zou, X. Chen, H. Deng, Q. Zhang and Y. Yan, *Materials*, 2024, **17**, 1861; https://doi.org/10.3390/ma17081861.
17 Z. Abbas, M. Dapporto, A. Tampieri and S. Sprio, *J. Compos. Sci.*, 2021, **5**, 259; https://doi.org/10.3390/jcs5100259.
18 I. I. Preobrazhenskiy and V. I. Putlyaev, *Mendeleev Commun.*, 2023, **33**, 531; https://doi.org/10.1016/j.mencom.2023.06.029.
19 L. D. C. Gutiérrez Púa, J. C. Rincón Montenegro, A. M. Fonseca Reyes, H. Zambrano Rodríguez and V. N. Paredes Méndez, *J. Mater. Sci.*, 2023, **58**, 3879; https://doi.org/10.1007/s10853-023-08237-5.
20 Ż. Ciosek, K. Kot, D. Kosik-Bogacka, N. Łanocha-Arendarczyk and I. Rotter, *Biomolecules*, 2021, **11**, 506; https://doi.org/10.3390/biom11040506.
21 A. M. Al Alawi, S. W. Majoni and H. Falhammar, *Int. J. Endocrinol.*, 2018, **1**, 9041694; https://doi.org/10.1155/2018/9041694.
22 S. R. Khan, M. S. Pearle, W. G. Robertson, G. Gambaro, B. K. Canales, S. Doizi, O. Traxer and H.-G. Tiselius, *Nat. Rev. Dis. Primers*, 2016, **2**, 1; https://doi.org/10.1038/nrdp.2016.8.
23 S. Zhang, L. Li and X. Lv, *J. Mater. Sci.: Mater. Electron.*, 2017, **28**, 1620; https://doi.org/10.1007/s10854-016-5703-y.
24 E. Vorndran, K. Wunder, C. Moseke, I. Biermann, F. A. Müller, K. Zorn and U. Gbureck, *Adv. Appl. Ceram.*, 2011, **110**, 476; https://doi.org/10.1179/1743676111Y.0000000030.
25 I. I. Preobrazhenskiy, D. V. Deyneko, V. V. Titkov, A. M. Murashko and V. I. Putlyaev, *Ceram. Int.*, 2023, **49**, 29064; https://doi.org/10.1016/j.ceramint.2023.06.182.
26 I. I. Preobrazhenskiy, Ya. Yu. Filippov, P. V. Evdokimov and V. I. Putlyaev, *Inorg. Mater.*, 2023, **59**, 500; https://doi.org/10.1134/S002016852305014X.
27 I. I. Preobrazhenskiy and V. I. Putlyaev, *Inorg. Mater.*, 2022, **58**, 349; https://doi.org/10.1134/S0020168522030128.
28 Z. Zhang, F. Zhou and E. J. Lavernia, *Metall. Mater. Trans. A*, 2003, **34**, 1349; https://doi.org/10.1007/s11661-003-0246-2.
29 A. K. Zak, W. H. A. Majid, M. E. Abrishami and R. Yousefi, *Solid State Sci.*, 2011, **13**, 251; https://doi.org/10.1016/j.solidstatesciences.2010.11.024.
30 D. Balzar, N. Audebrand, M. R. Daymond, A. Fitch, A. Hewat, J. I. Langford, A. Le Bail, D. Louër, O. Masson, C. N. McCowan, N. C. Popa, P. W. Stephens and B. H. Toby, *Appl. Crystallogr.*, 2004, **37**, 911; https://doi.org/10.1107/S0021889804022551.

Received: 26th December 2024; Com. 24/7716